ELSEVIER

Biochemical Pharmacology 63 (2002) 897–908

Biochemical Pharmacology

A doxorubicin–CNGRC-peptide conjugate with prodrug properties

Yvette van Hensbergen, Henk J. Broxterman*, Yvonne W. Elderkamp, Jan Lankelma, Judith C.C. Beers, Marc Heijn, Epie Boven, Klaas Hoekman, Herbert M. Pinedo

Department of Medical Oncology, Vrije Universiteit Medical Centre, P.O. Box 7057, 1007 MB Amsterdam, The Netherlands

Received 30 July 2001; accepted 13 November 2001

Abstract

There is increasing interest in the exploitation of molecular addresses for the targeting of tumor imaging or therapeutic agents. A recent study demonstrated anticancer activity in human xenografts of doxorubicin (DOX)–peptide conjugates targeted to the tumor vascular endothelium, among them DOX coupled to the cyclic pentapeptide CNGRC [Science 279 (1998) 377]. In order to learn more about the mechanism of action of this type of DOX–peptide conjugates, we have studied the interaction of DOX–CNGRC with primary human umbilical cord vein endothelial cells (HUVEC) and tumor cells under defined *in vitro* conditions. We used a DOX conjugate, in which the cyclic CNGRC peptide, for which an *in vivo* endothelial address has recently been identified as aminopeptidase N (APN)/CD13, has been coupled via a hydrolysable spacer to the C-14 anthracycline-side chain. First we determined that the $t_{1/2}$ of DOX–CNGRC conjugate in human blood was 442 min (at 37°) allowing sufficient time for endothelial targeting when administered i.v. When cultured cells were exposed for 30 min to DOX–CNGRC a more cytoplasmic localization of fluorescent drug was seen when compared to DOX exposure and intracellular DOX–CNGRC was identified after extraction from the cells. This revealed differences in the cellular uptake process of the conjugate compared to DOX. The antiproliferative effect of DOX–CNGRC was determined by 30 min exposure in medium with a high protein content in order to mimick the *in vivo* targeting situation. In this medium, the IC_{50} was 1.1 μM for highly CD13 expressing HT-1080, 1.45 μM for CD13 negative SK-UT-1 sarcoma cells and 6.5 μM for CD13 positive HUVEC. The IC_{50} of DOX for these cells were 1.0, 2.0 and 7.3 μM, respectively. Although DOX–CNGRC inhibited the peptidase activity of CD13 up to 50%, our data do not favor an important role for the enzyme inhibition in the cytotoxic effect of the conjugate. The antitumor activity was tested in nude mice bearing human ovarian cancer xenografts (OVCAR-3). A weekly i.v. administration (3 mg/kg DOX-equivalent, 3×) showed a minor (40%) growth delay, which does not indicate efficacy better than that expected for free DOX. In conclusion, this study indicates that the antiproliferative and anti-angiogenic effects of DOX–CNGRC as reported before, are likely caused by the cytostatic effects of intracellularly released parent drug DOX, independent of CD13 expression/activity. More research is needed to identify the optimal specific chemical configuration of DOX–peptide conjugates for *in vivo* targeting and receptor-mediated cellular uptake.

Keywords: Aminopeptidase N; CD13; Doxorubicin; Doxorubicin–peptide conjugate; Prodrug; Tumor vasculature

1. Introduction

DOX is a potent anticancer agent with activity in many solid tumors, among them breast cancer, small cell lung cancer and sarcoma. DOX was considered the most active single agent in metastatic breast cancer until the recent introduction of the taxanes [1]. Since the clinical introduction of the anthracyclines, daunorubicin and DOX in the early 1960s, it has been attempted to synthesize better anthracyclines than DOX. Despite the estimated synthesis of well in excess of 2000 analogs already in 1992 a truly better anthracycline has not been found [2].

Since DOX continues to be a widely used anticancer drug, there still is the need to improve the efficacy of its antitumor activity. One approach would be based on an improved delivery of the agent in tumors. The current increase in knowledge on tumor vascular biology and barriers to tumor drug delivery [3–5] as well as improvement of technologies for targeted delivery such as liposomal formulations [6] or by prodrug administration [7], suggest room for such an approach.

Along with the recent intense interest in the specific targeting of angiogenic tumor blood vessels, membrane

* Corresponding author. Tel.: +31-20-444-2607; fax: +31-20-444-3844.
E-mail address: h.broxterman@vumc.nl (H.J. Broxterman).

Abbreviations: DOX, doxorubicin; APN, aminopeptidase N; HUVEC, human umbilical cord vein endothelial cells.

0006-2952/02/$ – see front matter
PII: S0006-2952(01)00928-5

proteins overexpressed in endothelial cells of tumor microvessels have been identified, which may be candidates for imaging and therapeutic approaches. Membrane proteins, upregulated on proliferating endothelial cells include the VEGF-2 (Flk-1/KDR) receptor, $\alpha_v\beta_3$-integrin and the fibronectin isoform containing the ED-B oncofetal domain [8]. Also, recently the target of an *in vivo* phage tumor homing peptide, containing the NGR (asparagine–glycine–arginine) motif was identified as the APN or CD13 by Pasqualini *et al.* [9]. APN is a membrane-spanning, M_r 150,000 cell surface protein, expressed in various epithelial cells and in macrophages [10,11]. Importantly the only vascular structures with detectable APN are tumor blood vessels and other type of vessels undergoing angiogenesis, with the possible exception of cerebellar capillaries [12,13]. Moreover, APN antagonists, which inhibit its protease activity have anti-angiogenic properties [9,14].

The *in vivo* tumor-targeting properties of a peptide containing the NGR motif have been reported in two key papers by Arap *et al.* [15] and Ellerby *et al.* [16], in which a cyclic pentapeptide CNGRC with a disulfide bridge between both cysteines has been coupled to either DOX [15] or to a 14-amino acid pro-apoptotic peptide (KLAKLAKKLAKLAK) [16]. In both cases, the CNGRC tumor-homing peptide, but not a control CARAC peptide induced a marked increased antitumor effect in human breast cancer xenografts.

Altogether these data suggest that improved delivery of the potent antitumor drug DOX by vascular targeting to tumor endothelium may enhance its efficiency of tumor cell killing, either by improving the limited penetration of DOX in solid tumors [4] or by inhibiting the proliferation of tumor vascular endothelial cells. The latter possibility is even more attractive because it has been shown recently that low doses of chemotherapy may have antitumor effect independent from direct effects on the tumor cells [17–19]. However, the original study describing the antitumor effect of cyclic peptide-targeted DOX does not address these questions [15].

Therefore, in this study, we have explored the *in vitro* interaction of a DOX–peptide conjugate with HUVEC and tumor cells. Arap *et al.* [15] describe two types of conjugates prepared by a different chemistry and with a similar antitumor activity (see [18] in Arap *et al.* [15]). One conjugate is a mixture of undefined reaction products, which hampers further characterization. Here we used the second DOX–CNGRC conjugate, synthesized by a chemistry that (a) allows to make a stoichiometrically defined conjugate; and (b) may act as DOX prodrug by introducing a hydrolysable spacer.

We determined the stability of the DOX–CNGRC conjugate in human blood and plasma as well as its effects on the APN enzymatic activity. Then the *in vitro* cytotoxicity of the conjugate for HUVEC and tumor cell lines with low or high CD13 expression was measured under conditions, mimicking the *in vivo* situation in blood and the *in vivo* antitumor effect was tested in a human ovarian cancer xenograft.

2. Materials and methods

2.1. Cells

HUVEC were isolated and cultured from single umbilical cords that were stored in cord buffer at 4° for 1–7 days essentially according to procedures described extensively before [20]. Briefly, HUVEC were harvested by incubating the vein with trypsine/EDTA solution for 20 min at 37°. HUVEC were cultured in fibronectin (2 μg/mL) coated 6-well plates (Costar) in M199 medium (Gibco) containing 10% pooled human serum, 10% fetal calf serum (Gibco), 5 unit/mL heparin, 200 μg/mL penicillin and 200 μg/mL streptomycin, 290 mg/mL L-glutamine and 50 μg/mL crude endothelial cell growth factor, isolated from bovine brain [20]. HUVEC were used for experiments after passage 1 or 2.

The human tumor cell lines HT-1080 (fibrosarcoma), SK-UT-1 (mixed mesodermal tumor) and SK-LMS-1 (leiomyosarcoma), WLS-160 (liposarcoma), MCF-7 and KB3-1 (carcinomas) were cultured in Dulbecco's MEM (BioWhittaker) with 10% fetal calf serum. Growth inhibition was measured in an MTT-assay in 96-well plates. 3000 HUVEC or 2500 tumor cells were seeded per well and allowed to recover overnight. Then the cells were exposed to drug 30 min in the indicated medium (eight drug concentrations, 3-well per concentration, 6-well for controls), drug was washed away and the cells were cultured for 72 hr in full growth medium. Then viable cells were determined by a standard MTT-assay. The IC_{50} (50%) growth inhibitory concentrations were calculated of four to six experiments (SK-UT-1, three experiments) for different HUVEC isolates (and HT-1080 determined in parallel). HUVEC were done more than three times in order to ensure more representative results from different isolates.

2.2. Chemicals/drugs

2.2.1. Doxorubicin

Dox.HCl (Adriblastine R.T.U.) was from Pharmacia & Upjohn and was stored as a 3.1 mM solution in saline at −20°. Doxorubicin–Cys–Asn–Gly–Arg–Cys–NH_2 (DOX–CNGRC) and doxorubicin–Cys–Ala–Arg–Ala–Cys–NH_2 (DOX–CARAC) and CNGRC with a disulfide bridge between both cysteines, were synthesized by AnaSpec Inc. DOX was conjugated via C-14 to CNGRC by an amide bond between a carboxyl group of an N-Fmoc-doxorubicin-14-*O*-hemiglutarate and the amino group of the peptide, according to Nagy *et al.* [21]. The presence of the conjugate and of free DOX were identified by LC–MS by the manufacturer and checked again upon arrival. The HPLC purity of two separate preparations was according to

the manufacturer >90 and >95%, respectively, and was checked by us and found to be 94 and 98%, respectively. The DOX-conjugates were dissolved in Milli-Q water (200 μM–1 mM) and stored at −20°. During our experiments, we have continuously monitored the stability of the stocks as well as free DOX present, which remained always <5% upon storage.

2.3. HPLC analysis

The purity and breakdown of the conjugate under several conditions was monitored by HPLC analysis and spectrofluorometric detection after extraction in 67% acetonitrile. For the extraction of DOX–CNGRC from cells, a method with improved extraction efficiency for anthracyclines was employed [22,23]. The cell pellet was resuspended and vortexed in 50 μL H_2O, then 50 μL of 20 mM H_3PO_4 1 mM saccharolactone (pH = 3.0; Sigma) and 10 μL 3.3% (v/v) $AgNO_3$ + 40 μL acetronitrile were added. The material was sonicated for 10 min in a waterbath and centrifugated for 3 min at 14,000 rpm in an eppendorf centrifuge [23]. The separation was performed by isocratic elution (25% acetonitrile, 75% HPLC buffer, consisting of 10 mM tri-ethylamine, 10 mM NaH_2PO_4, pH = 3.5) with a flow rate of 1 mL/min on an Absorbosphere HS C18, 3 μm particle column (Alltech) with a LiChroCART4-4/Lichrospher 100 RP-18, 5 μm guard column (Merck). Detection was by diode-array (220 nm) and spectrofluometry at λ_{exc} of 475 nm and λ_{em} of 551 nm. The human plasma and serum were collected from healthy volunteers in standard vacutainers. Whole blood and platelet-poor plasma (ppp) were obtained by venipuncture in syringes containing 0.11 mol/L sodium citrate, 1.4 g/100 mL citric acid and 2 g/100 mL glucose.

2.4. CD13 expression

Log phase cells were harvested by short trypsinization, washed and suspended in buffered medium, containing 10% FCS. Briefly, 1×10^5 cells were incubated at room temperature for 60 min with FITC-conjugated anti-human CD13 monoclonal antibody WM-47 (5 μg/mL; DAKO) or FITC-conjugated mouse-IgG1 (DAKO). The cells were washed and analyzed on a FACS Calibur flow cytometer (Becton Dickinson). The results are expressed as ratios of mean fluorescence of WM-47 divided by IgG1 control.

2.5. Immunohistochemistry

Cryostat tissue sections (4 μm thick) of OVCAR-3 xenograft tumors were mounted on poly-L-lysine coated slides and fixed with acetone. Staining for mouse CD13 was done with the rat ER-BMDM-1 antibody (kind gift of P.J. Leenen, Department of Immunology, Erasmus University, Rotterdam, The Netherlands), followed by incubation with peroxidase-labeled secondary antibody. Staining for PECAM-1 was performed with goat polyclonal anti-PECAM-1 antibody (Santa Cruz). For color development, the slides were incubated with biotin-labeled rabbit-anti-goat and peroxidase-labeled streptavidin and 0.05% 3,3′-diaminobenzidine tetrahydrochloride dihydrate containing 0.02% H_2O_2. Slides were counterstained with hematoxylin. In the negative controls, the primary antibody was omitted. Mouse liver was used as a positive control for CD13 and showed staining of the bile canaliculi.

2.6. Laser scanning microscopy

The intracellular localization of fluorescent DOX and conjugate was determined on a laser scanning microscope (Leica TCS 4D) using a krypton:argon laser (λ_{exc} of 488 nm and λ_{em} of 590 nm) and a 40× oil lens [24]. Cells (25,000) were seeded on coverslips (for HUVEC coated with fibronectin) and grown overnight. Then the cells were incubated with DOX or conjugate and examined after the indicated times.

2.7. Aminopeptidase assay

Membrane preparations of HT-1080 and SK-UT-1 cells were isolated. In short, cells were resuspended in buffer (100 mM KCl, 50 mM Hepes pH 7.4, 5 mM $MgCl_2$, 1 mM PMSF) and incubated for 1 hr at 0°. After sonification, the membranes were isolated by centrifugation on 46% sucrose and resuspended in buffer. HT-1080 (1 μg) and SK-UT-1 (25 μg) membranes were incubated at 37° with 15 μM Alanine–MCA (L-alanine-4-methyl-7-coumarinylamide trifluoroacetate, Fluka) in PBS, pH 7.2 in a 96-well plate in triplo. The activity blocking antibody WM-15 [25] (5 μg/mL; Pharmingen) was used to determine the CD13-specific aminopeptidase activity. The development of the fluorescent product 7-AMC was monitored automatically every 5 min on a Spectrafluor multiplate reader (Tecan) (λ_{exc} of 360 nm and λ_{em} of 465 nm) and was linear up to at least 90 min. To determine the surface aminopeptidase activity of intact cells, 5000 cells per well were plated in a 96-well plate and left overnight in medium with 1% FCS. Then the cells were incubated with 100 μM alanine–MCA in PBS, 0.5% bovine serum albumin (BSA), pH = 7.2. The aminopeptidase activity was calculated from the slope of the fluorescence-time curve, using a calibration curve of 7-AMC (Fluka).

2.8. Antitumor activity in vivo

The animal experiment was approved by the Institution Animal Experiments Committee and performed in accordance with the institution guidelines. Female athymic nude mice, 8–10-week-old (Hsd: athymic nude-*nu*; Harlan Cpb.) were transplanted with 2–3 mm tumor tissue fragments from previous recipients bearing OVCAR-3 human ovarian cancer xenografts. OVCAR-3 shows a poorly differentiated

serous adenocarcinoma histology and tumors have a volume-doubling time of approximately 5 days. Upon growth, tumors were measured and mice were weighed twice a week throughout the entire experiment. The tumor volume was calculated by length × width × thickness × 0.5. Treatment was started at the time tumors had a mean volume of 180 mm^3. For evaluation of DOX–CNGRC effect, the relative tumor volume was expressed by the formula V_T/V_0, where V_T is the volume on any given day and V_0 is the volume on day 0. The ratio between the mean of the relative volumes of treated tumors and that of control tumors × 100% (T/C%) was used to express the growth inhibition calculated as 100% − T/C% [26].

2.9. Statistics

Statistical analysis of cytotoxicity and aminopeptidase data was done by Student's *t*-test, performed using SPSS software (SPSS Inc., Chicago, IL).

3. Results

3.1. DOX–CNGRC stability

The cyclic pentapeptide CNGRC has been shown to selectively target tumor endothelium in xenografts [15,16]. We have studied the interaction of DOX–CNGRC (structure is shown in Fig. 1), with HUVEC and with tumor cells in relation to CD13 expression of the cells.

However, first the stability of the conjugate was measured upon incubation at 37° in cell culture medium and in human whole blood, plasma and serum in order to mimick conditions after systemic administration. The results are shown in Table 1 and Fig. 2. The stability of the conjugate was highest in human whole blood ($t_{1/2} = 442$ min) or platelet-poor plasma ($t_{1/2} = 296$ min). It shows an almost similar stability in PBS containing 4 g/100 mL BSA (pH = 7.2) ($t_{1/2} = 213$ min). In contrast, a faster hydrolysis into DOX is seen in human serum or plasma ($t_{1/2} < 60$ min) or cell culture medium ($t_{1/2} \approx 75$ min). The only fluorescent degradation product identified by HPLC was the parent drug DOX. Also no linearization of the peptide occurred in the medium during these incubations, as appeared from the absence of any detectable HPLC peak corresponding to the one rapidly occurring after incubation of the conjugate with 1 mM dithiothreitol. The stability of the conjugate in PBS/BSA or in cell culture medium increased with decreasing pH. In a typical experiment, during a 30 min incubation in PBS/BSA of pH 7.6, 7.2 and 6.8, 17, 7 and 4% of the conjugate turned into DOX, respectively.

Table 1
Degradation of DOX–CNGRC at 37°

Medium	k (min^{-1})	$t_{1/2}$ (min)	n
Whole human blood	0.0016 ± 0.00013	442 ± 39	3
Platelet-poor plasma	0.0026 ± 0.00014	296 ± 21	6
Citrated plasma	0.0157 ± 0.00062	46 ± 2	5
Human serum	0.0146 ± 0.0013	53 ± 5	4
PBS + 4% BSA (pH = 7.2)	0.0033 ± 0.00014	213 ± 10	3
DMEM + 10% FCS	0.0094 ± 0.00072	76 ± 6	3

The degradation rate constant (k) was calculated from the ln[DOX–CNGRC] vs. time curve (according to $C_t = C_0 \times e^{-kt}$). The $t_{1/2}$ values longer than 200 min are based on 90 min experiments and added for comparison. Data are mean ± SE.

3.2. DOX–CNGRC cytotoxicity

In order to compare the cytotoxic effects of DOX–CNGRC with DOX, we selected HUVEC and two human sarcoma cell lines, based on a high CD13 expression (HT-1080) and no CD13 expression (SK-UT-1) as determined from a small panel of cell lines (Fig. 3).

The growth inhibitory effect of DOX–CNGRC was determined by a 30 min incubation followed by a 72 hr drug-free period in order to simulate short-duration *in vivo* exposures and because of the relative unstability of the conjugate in cell culture medium. The average free DOX concentration during this incubation period was 17% of DOX–CNGRC. In order to further limit the effect of free DOX, we have also exposed the cells to the conjugate in PBS/BSA for 30 min. In that medium, the stability is relatively high and mimicks that in human whole blood

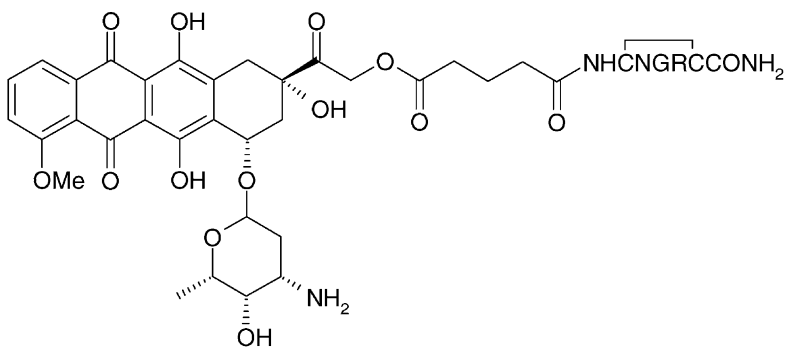

Fig. 1. Chemical structure of the DOX–CNGRC conjugate.

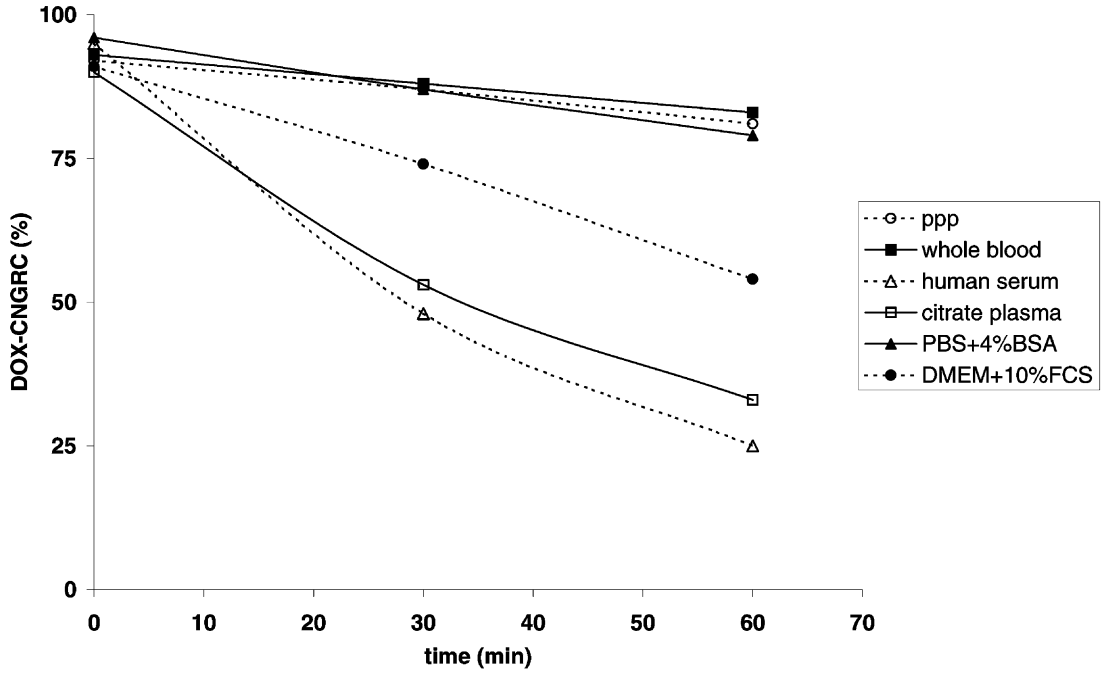

Fig. 2. Degradation of DOX–CNGRC (4 μM) in different media (for number of experiments and SE, see Table 1).

(the average free DOX concentration was 7% of the DOX–CNGRC concentration).

Table 2 shows the IC_{50} data for DOX and DOX–CNGRC. The IC_{50} for DOX are higher in PBS/BSA than in cell culture medium. This can be explained by a lower cellular uptake rate of DOX in PBS/BSA because of a lower pH and higher protein binding compared to cell culture medium. From the IC_{50}, we conclude that DOX–CNGRC is less cytotoxic than DOX in cell culture medium, but has almost the same cytotoxicity in PBS/BSA. Since in the latter medium an average of only 7% of the total (free + conjugated) DOX was free DOX during the incubation

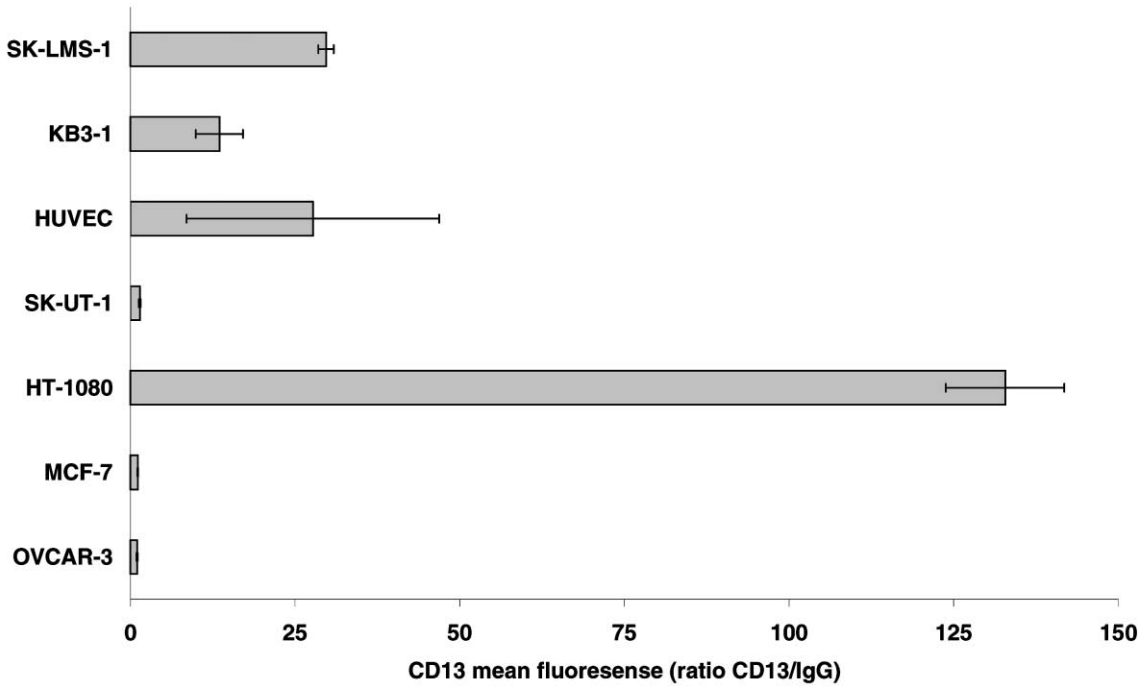

Fig. 3. CD13 expression in selected cell lines. Data represent mean ± SD of at least three experiments per cell line and for HUVEC, 11 different isolates were tested.

Table 2
Cytotoxicity of DOX and DOX–CNGRC

Cell line	IC_{50} [DOX] (μM)		IC_{50} [DOX–CNGRC] (μM)	
	Medium	PBS/BSA	Medium	PBS/BSA
HUVEC	2.7 ± 1.0 ($n = 6$)	7.3 ± 1.3 ($n = 4$)	18.6 ± 8.1 ($n = 6$)	6.5 ± 1.3 ($n = 4$)
HT-1080	0.21 ± 0.06 ($n = 5$)	0.96 ± 0.36 ($n = 5$)	1.21 ± 0.24 ($n = 6$)	1.12 ± 0.71 ($n = 6$)
SK-UT-1	0.94 ± 0.48 ($n = 3$)	1.98 ± 0.76 ($n = 3$)	5.21 ± 0.94 ($n = 3$)	1.45 ± 0.62 ($n = 3$)

IC_{50} (50% growth inhibitory concentrations) are mean ± SD of n independent experiments; 30 min drug exposure followed by a 72 hr drug-free period. PBS/BSA is PBS containing 4 g/100 mL BSA, pH = 7.2. All IC_{50} of DOX in medium were statistically lower than the IC_{50} of DOX–CNGRC in medium ($P < 0.01$ for HUVEC and HT-1080; $P < 0.05$ for SK-UT-1). No significant differences between both drugs were seen in PBS/BSA.

period (increasing from 2.5% at time zero to 11.5% at $t = 30$ min) it is clear that DOX–CNGRC itself is the major drug molecule that interacts with the cells and after uptake and probably cleavage, has growth inhibitory activity. Moreover, the different behavior in both media (DOX less effect, but DOX–CNGRC more effect in PBS/BSA) is indicative for different processes involved in the cellular uptake of parent drug and conjugate. This was further substantiated by adding a 250-fold excess of cyclic peptide CNGRC to DOX–CNGRC (1 μM) to HT-1080 cells. CNGRC decreased the growth inhibitory effect of DOX–CNGRC from 65 to 32% (mean of two experiments). In contrast no effect was seen on DOX-induced growth inhibition.

3.3. DOX–CNGRC intracellular localization

The fluorescence of the DOX fluorophore allows to visualize differences in intracellular localization after exposure of cells to DOX or DOX–CNGRC. In these experiments, we have compared 4 μM DOX–CNGRC with 2 μM DOX, because the fluorescence quantum yield of the conjugate was about 50% of the parent drug. Fig. 4B shows that the fluorescence distribution in HT-1080 cells exposed for 30 min to DOX–CNGRC is clearly in favor of a cytoplasmic and perinuclear localization, whereas DOX is preferentially localized into the nucleus (Fig. 4C). The contribution of uptake from a small amount of free DOX as present in DOX–CNGRC cannot be clearly discriminated from the autofluorescence background at this time-scale (Fig. 4A). After incubation periods of 60 min or longer, a clear nuclear fluorescence localization becomes predominant in DOX–CNGRC incubated cells as well (not shown). By *in vitro* binding to calf thymus DNA, we found that DNA quenched the fluorescence of 1 μM DOX–CNGRC and DOX to the same extent, namely 95–97% at 25 μg/mL DNA. This indicates similar DNA binding properties and hence potential nuclear localization properties for both drugs. The more predominant localization into cytoplasmic structures of DOX–CNGRC compared to DOX resembles that seen with more lipophilic anthracyclines such as idarubicin. Indeed, DOX–CNGRC is more lipophilic than DOX as determined from their 1-octanol/PBS (pH = 7.4) distribution ratios, which were 5.3 and 1.2, respectively. From preliminary experiments, it appeared that the extraction of DOX–CNGRC from cell material was less efficient than the extraction of DOX, also with the improved extraction method [23]. Still we could clearly identify DOX–CNGRC in cells after incubation for 30 min with 8 μM DOX–CNGRC. In two experiments, the intracellular amount of DOX–CNGRC was 281 and 154 pmol/10^6 HT-1080 cells, while intracellular DOX was 7.1 and 1.5 pmol/10^6 cells, respectively, proving that the cytoplasmic localized fluorescence as seen with fluorescence microscopy was indeed for at least 95% DOX–CNGRC at this time-point. When the drug in the medium was washed out after 30 min and the cells were left, the intracellular DOX–CNGRC levels decreased with a concominant increase in DOX (not shown).

The CD13 activity blocking antibody WM-15 had no effect on the fluorescence distribution of DOX–CNGRC in HT-1080 cells (Fig. 4D), suggesting that the enzymatic activity of CD13 was not necessary for the cellular uptake of DOX–CNGRC.

The subcellular fluorescence distribution in SK-UT-1 (not shown) and HUVEC (Fig. 4E–J) after 30 min exposure to DOX or DOX–CNGRC shows a similar distribution pattern as in HT-1080 cells. DOX–CNGRC has a more punctate, cytoplasmic pattern (Fig. 4F) compared to the predominant nuclear DOX fluorescence (Fig. 4G). Despite the high quenching factor by nuclear DNA, nuclear DOX fluorescence can be seen faintly after 30 min exposure of HUVEC to a concentration as low as 400 nM DOX in cell culture medium (Fig. 4H). Similarly, also nuclear fluorescence after exposure to 2 μM DOX can already be seen after 5 min.

Instead, a much higher concentration of DOX–CNGRC, than can be accounted for by the 50% lower quantum yield, is necessary to clearly see fluorescence above background in the nucleus. These data, therefore, show that the DNA-bound fluorescence appears slower after exposure of cells to DOX–CNGRC than to DOX. In addition, in PBS/BSA the uptake of DOX is clearly less than in endothelial culture medium (compare Fig. 4G and I), consistent with the cytotoxicity data. For DOX–CNGRC, this is more difficult to see (Fig. 4F and J), because the DOX–CNGRC fluorescence is mainly in the cytoplasm where the cellular autofluorescence background is higher than in the nucleus.

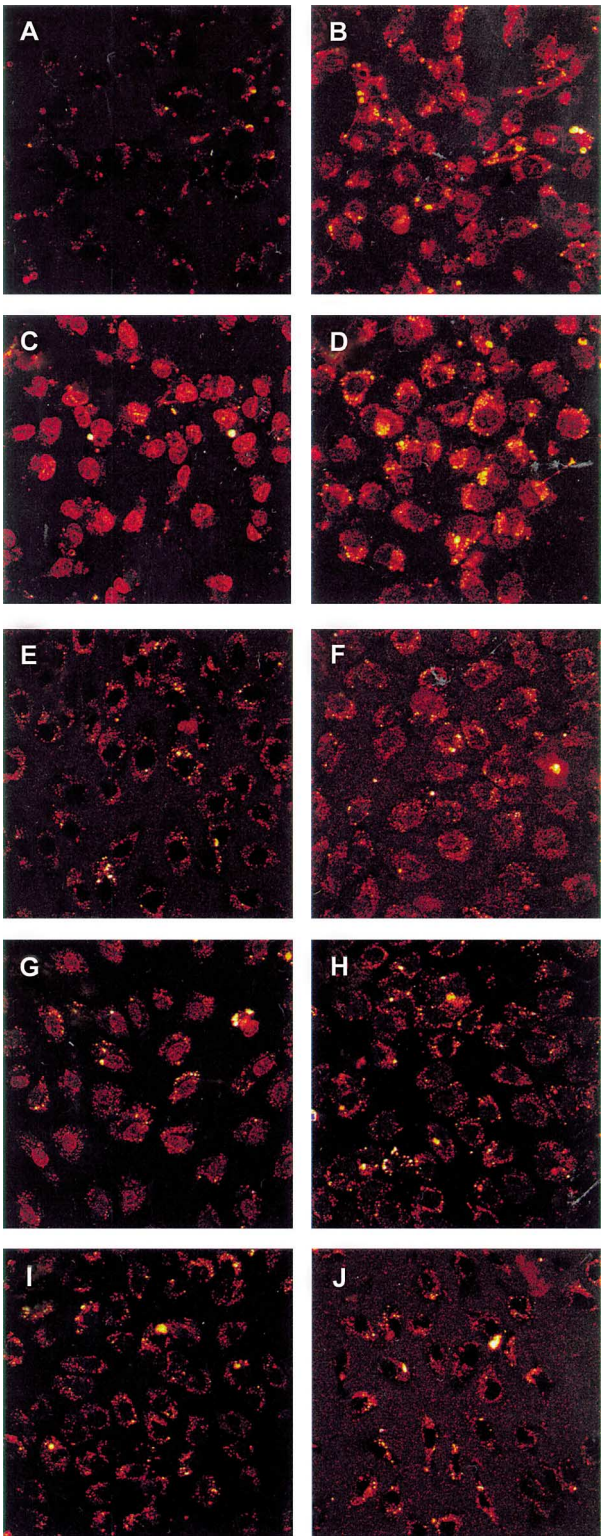

Fig. 4. Intracellular fluorescence after 30 min exposure of HT-1080 (A–D) and HUVEC (E–J) to DOX–CNGRC or DOX. (A) HT-1080, autofluorescence of cells; (B) HT-1080, 4 μM DOX–CNGRC in DMEM; (C) HT-1080, 2 μM DOX in DMEM; (D) HT-1080, 4 μM DOX–CNGRC + 2.5 μg/mL WM-15 in DMEM; (E) HUVEC, autofluorescence; (F) HUVEC, 4 μM DOX–CNGRC in endothelial medium; (G) HUVEC, 2 μM DOX in endothelial medium; (H) HUVEC, 0.4 μM DOX in endothelial medium; (I) 2 μM DOX in PBS/BSA; (J) HUVEC, 4 μM DOX–CNGRC in PBS/BSA.

Summarizing, after short-term exposure (30 min in this case) DOX–CNGRC is more localized into the cytoplasm and less prominent into the cell nucleus compared to DOX.

3.4. DOX–CNGRC effects on CD13 activity

The aminopeptidase activity of intact cells was determined by measuring the fluorescence development after hydrolysis of the substrate alanine–MCA. The CD13 specificity was determined as the amount of activity blocked by the antibody WM-15 [25]. The percentage of CD13 activity of the total aminopeptidase activity was highest in HT-1080 (57%), 26% in HUVEC (mean of five different isolates) and between 10 and 20% for the other tumor cell lines. The correlation of CD13 expression with CD13 activity in the cell lines was high ($R = 0.996$; $P < 0.001$). In order to test the effects of drugs on the CD13 activity, we prepared membrane fractions of HT-1080 cells, because in these cells the CD13 activity in absolute value and as percentage of total the aminopeptidase activity was the highest. In HT-1080 membranes WM-15 inhibited 80% of the aminopeptidase activity at 2.5 μg/mL (Fig. 5a), possibly because the antibody has better access to its binding site in membrane preparations compared to intact cells. Subsequently, it was shown that 2.5 μM DOX–CNGRC inhibited 9% of the CD13 activity, which increased to 42% at 20 μM. In contrast, DOX had no effects up to 20 μM tested (see Fig. 5b). Also the cyclic peptide CNGRC had no effect up to 300 μM (highest concentration tested, not shown). Fig. 5c summarizes the effects of all tested drugs and combinations. DOX–CNGRC and DOX–CARAC (20 μM) inhibited about 50% of the aminopeptidase activity, whereas DOX (20 μM), CNGRC (100 μM) or both added together, but not conjugated, had no significant effect. DOX–CNGRC further increased the inhibitory effect when tested together with an optimal concentration of WM-15 (93% inhibition with DOX–CNGRC + WM-15 vs. 82% with WM-15: $P < 0.01$). This effect on the aminopeptidase activity that is not blocked by WM-15 could mean that WM-15 may not fully block the enzymatic activity of CD13 or that DOX–CNGRC has also some effect on another membrane aminopeptidase such as cystinyl aminopeptidase/oxytosinase.

3.5. DOX–CNGRC antitumor effects on OVCAR-3 xenografts

In order to test the potentially high efficacy and low toxicity of this conjugate which has a 1:1 stoichiometry of DOX coupled to CNGRC, we performed an *in vivo* experiment. This product was claimed in the original publication to have a similar high efficacy to a carbodiimide conjugate and much higher efficacy than free DOX ([15], note [18]). We have used the OVCAR-3 xenografts because according to our experience it has a very reproducible tumor growth

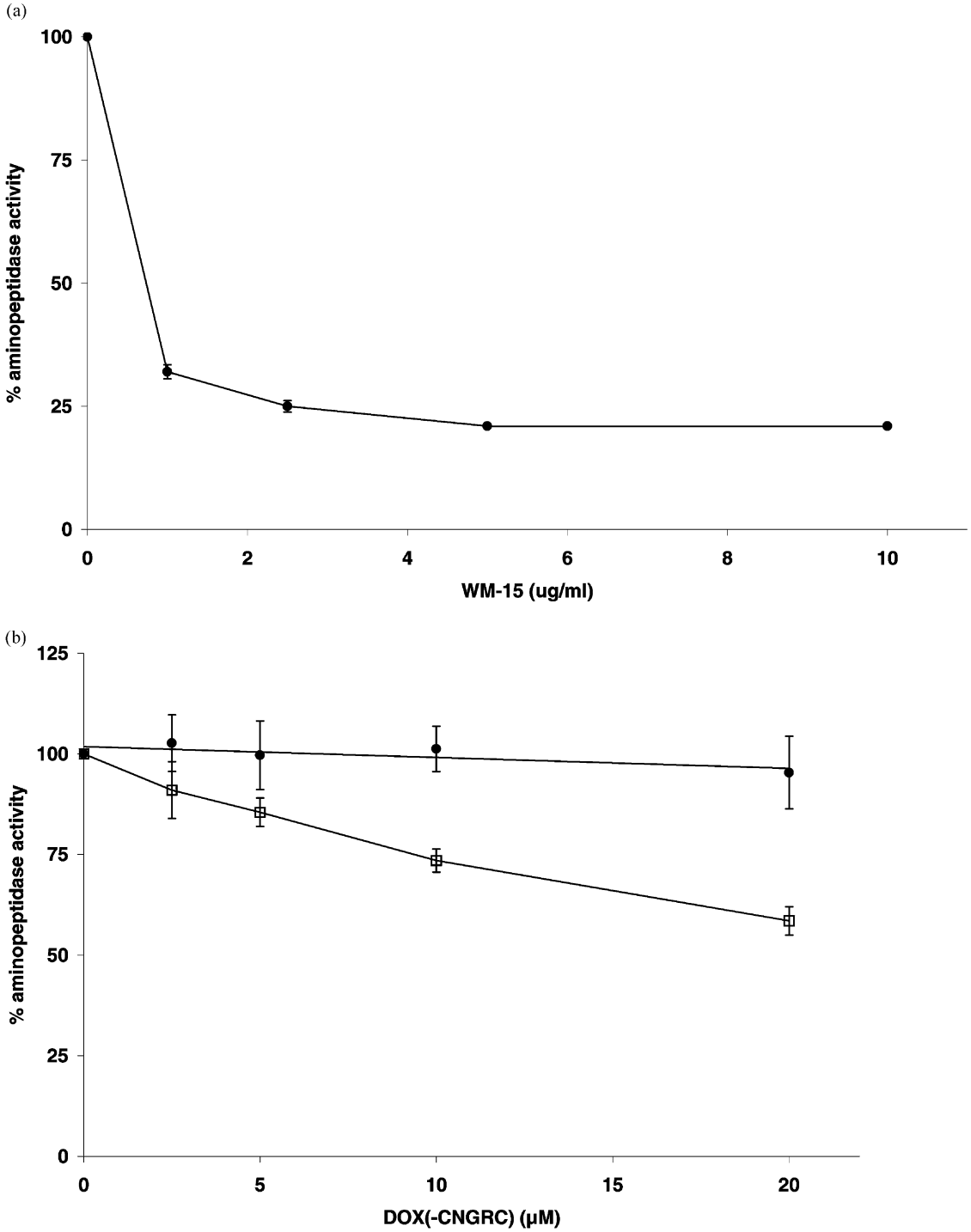

Fig. 5. (a) Concentration–effect curves of aminopeptidase inhibition in HT-1080 membranes of WM-15; (b) DOX (●) and DOX–CNGRC (□); (c) the inhibitory effects of 20 μM DOX, DOX–CARAC and DOX–CNGRC; 100 μM CNGRC; 5 μg/mL WM-15. The asterisk (∗) significantly different from control ($P < 0.005$; Student's *t*-test).

in which we have ample experience in testing DOX and DOX-derivatives [26,27]. Moreover, at the MTD of 8 mg/kg DOX (i.v., weekly 2×) a moderate, but highly consistent 60–65% tumor growth inhibition is seen [26]. Since this tumor shows a moderate response to DOX, it is very useful to establish the effect of a putatively more efficacious analog. We have chosen a treatment schedule of one i.v. injection weekly during 3 weeks according to Arap *et al.* [15]. In order to observe enhanced efficacy, based on Arap *et al.* [15] we choose a dose that would be hardly effective as free DOX: 3 mg/kg DOX-equivalent. In Fig. 6, we demonstrate that a maximal growth inhibition of 40% was seen 18 days after the start of treatment, which cannot be regarded as a significant antitumour effect [27].

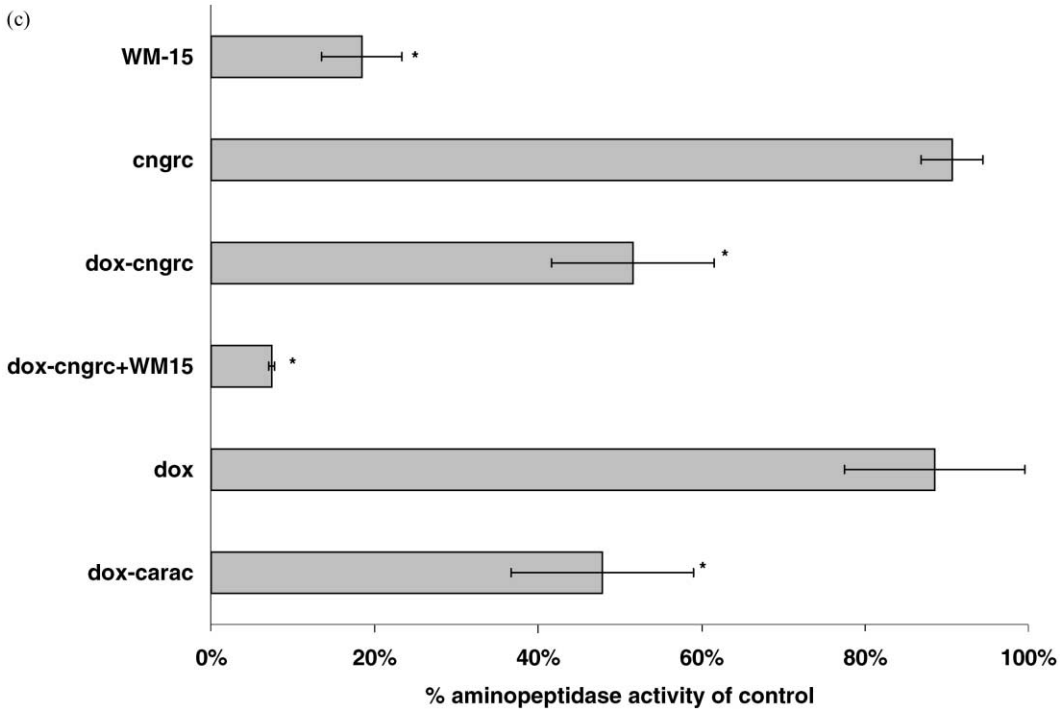

Fig. 5. (*Continued*).

The presence of CD13 expression in the OVCAR-3 xenografts was verified with the anti-mouse CD13 antibody ER-BMDM-1 [28]. PECAM-1 antibody showed the presence of endothelial cells in small capillaries as well as larger vessels. Positive staining with ER-BMDM-1 was observed in the mouse endothelial cells. No staining of endothelial cells or OVCAR-3 tumor cells was seen with the anti-human CD13 antibody WM-15, confirming the nearly absence of CD13 expression seen *in vitro*. In addition to the mouse endothelial cells also the stroma surrounding the vessels showed ER-BMDM-1 positive cells. Most likely these are fibroblasts, smooth muscle cells and/or pericytes, which are known to express CD13 [13,29]. These results are in line with the findings reported by Pasqualini *et al.*, who found co-localization of CD13 with APA, a marker of pericytes and smooth muscle cells [9].

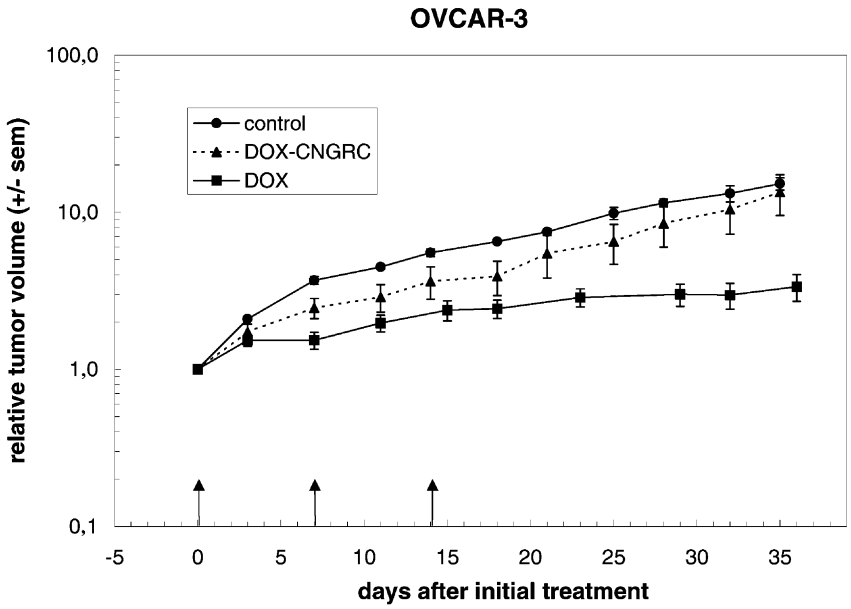

Fig. 6. Tumour growth in mice bearing OVCAR-3 xenografts after i.v. treatment with DOX–CNGRC (3 mg/kg DOX-equivalent, days 0, 7 and 14) or DOX (8 mg/kg, days 0 and 7). Data are from three mice per group with a tumor in both flanks.

4. Discussion

The cyclic NGR containing peptide, CNGRC, has been shown to home specifically and more effectively to tumors than linear peptides containing the NGR motif [15]. Since the NGR motif resembles the RGD motif, it was initially hypothesized that the receptor for CNGRC might be an integrin. By competition experiments, it was found that the ligand for α_v-integrins, the cyclic RGD-4C peptide did not compete with CNGRC, indicating that the receptor might be a different protein [15]. Indeed the receptor for cyclic CNGRC has been recently identified as being the aminopeptidase N/CD13 [9], which was found to be highly expressed in mouse as well as in human tumor endothelium [9]. Consistent with a preferential tumor vasculature localization, it has been found that CNGRC coupled to various cytotoxic agents had highly improved antitumor activity, in several xenograft models [15,16].

In order to increase our understanding of the properties of peptide-drug conjugates [30–33], we have studied the interaction of DOX–CNGRC with tumor and endothelial cells. Arap *et al.* [15] report the preparation of conjugate by two different chemical methodologies to couple CNGRC to DOX. One method used carbodiimide/*N*-hydroxysuccinimide chemistry, which yields a mixture of conjugates, precluding determination of the stoichiometry of the conjugate by mass spectrometry [15]. The other method used N-Fmoc chemistry to couple the peptide-amino group via a hemiglutarate spacer to the C_{14} side chain of DOX. This method was chosen by us, because Nagy *et al.* [21] showed that conjugates of DOX with a peptide hormone (LHRH), prepared with this chemistry (a) give a satisfactory yield of HPLC purified product; (b) preserve completely the cytotoxicity of DOX; and (c) fully retain the receptor binding affinity of the targeting peptide [21].

Indeed, we found in two preparations the predicted product to be >95 and >98% of the fluorescent products present, with free DOX accounting for the remainder. Importantly this conjugate has a good solubility in water. We found that the stability of the DOX–CNGRC conjugate was highly dependent on the matrix in which it was dissolved. In particular in serum containing matrix (cell culture media or 100% human serum) the half-life of the conjugate at 37° was shorter ($t_{1/2}$ of 45–75 min) than in human platelet-poor plasma and human blood ($t_{1/2}$ of 5–7 hr). This is not unexpected because serum may contain cell-derived esterase activity which can hydrolyze the conjugate. The only fluorescent hydrolysis product appearing during these incubations was the parent drug DOX. It appears from our experiments that a high protein content and a low pH, at least within the investigated range of pH 6.8–7.6, protect the conjugate against hydrolysis.

Because the specific homing of CNGRC expressing phages in the tumor vasculature of tumor-bearing mice was already seen after a short *in vivo* circulation time of only several minutes, the stability in the general circulation as estimated here from incubation in human whole blood, would be high enough to allow the targeting process to occur. Since in tumor blood vessels a coagulation-prone situation may exist [34], with locally higher concentrations of proteases and esterases, this more ''serum-like'' situation might lead to increased formation of free DOX in tumor tissue. In order to test whether we could reproduce the original findings on the high antitumour efficacy of DOX–CNGRC we had to make some choices. Since the enhanced *in vivo* effect was hypothesized to relate to mouse endothelial cell CD13 expression and was independent on CD13 expression of the tumor cells [15], we reasoned that we could use in principle any tumor xenograft, provided that it had some, but not too high sensitivity to DOX. According to our experience [26,27] OVCAR-3 xenografts would satisfy this criterion. Second, the administered dose should be lower than an effective dose of DOX, which is 8 mg/kg [26,27] in this model, also in order to exclude major effects of DOX itself which are to be expected because of hydrolysis of the conjugate after extended circulation, when a high DOX-equivalent dose is chosen. Since Arap *et al.* [15] reported a distinct antitumor effect already at 5 μg DOX-equivalent per mouse, (i.v. weekly 3×) the dose should be in between 5 and 160 μg DOX-equivalent per week (8 mg/kg) for a 20 g mouse. We have chosen 60 μg DOX-equivalent per week (3 mg/kg DOX-equivalent) which should be high enough to find an enhanced DOX effect similar to that found by Arap *et al.* [15] if it were present. While we did not find such an effect it remains possible that in other tumor models a higher efficacy can be found. Although CD13 was expressed in the mouse vasculature of OVCAR-3 xenografts, perhaps tumors with a different vascularization pattern or other administration schedules would be more appropriate. However, our *in vivo* experiment argues against a general applicability and/or the present conjugate does not have the optimal chemistry for a prodrug at least in this nude mouse model.

Table 2 shows that in PBS/BSA, DOX–CNGRC had a very similar IC_{50} as DOX for HUVEC as well as tumor cells. Thus, exposure of cells to DOX–CNGRC is cytotoxic in itself in the same concentration range as the parent compound. Still the behavior in different media shows a different tendency: DOX is less cytotoxic in PBS/BSA, a medium with a higher protein content and slightly lower pH, whereas the DOX–CNGRC cytotoxicity seems to be higher in PBS/BSA, where it is more stable. These differences in cytotoxicity between both drugs probably reflect at least in part the differences in the mechanism of intracellular uptake and localization of the drugs. Compared to DOX, the conjugate is initially more localized in the cytoplasm, possibly in endosomal-like and Golgi-related structures. Thus, the mechanism of plasma membrane passage and subsequent intracellular routing differs between both drugs. It will have to be studied further in

kinetic and mechanistic experiments what the relative contributions of passive diffusion and receptor-mediated uptake for DOX–CNGRC are in different cell types. The latter mechanism is suggested to contribute to the uptake, because an excess of peptide partly reversed the growth inhibitory effect of DOX–CNGRC. Other still ill-defined mechanisms of membrane translocation of peptides and coupled cytotoxics into mammalian cells may also play a role [35].

At later time-points during the exposure of cells to the conjugate, the fluorescence distribution in the cells becomes predominantly nuclear and looks more like the DOX fluorescence pattern. Abundantly present cellular esterases will result in intracellular hydrolysis of DOX–CNGRC to DOX. Since, however, also DOX–CNGRC itself binds to DNA, a contribution of the conjugate itself to the nuclear fluorescence and the DNA-intercalation/binding-induced antiproliferative action cannot be excluded.

The role of CD13 in the uptake and/or cytotoxicity of DOX–CNGRC has been investigated by several approaches. Pasqualini *et al.* [9] have shown that phages expressing CNGRC bound specifically to immunocaptured CD13 and to CD13 overexpressing tumor cells. Also they showed, that anti-CD13 antibody strongly inhibited the tumor homing of CNGRC phages in xenograft bearing mice. Here we show that the CD13 enzymatic activity blocking antibody WM-15 had no apparent effect on the uptake and intracellular localization of DOX–CNGRC into the highly CD13 expressing HT-1080 cells. In addition, the localization and cytotoxicity of DOX–CNGRC in HT-1080, intermediate CD13 expressing HUVEC and CD13 negative SK-UT-1 cells is rather similar, indicating that the process of uptake into cells, routing or possible processing to free DOX was not dependent on the level of CD13 expression. This is also substantiated by the finding that another cyclic pentapeptide, CARAC, when coupled to DOX, shows a similar pattern of fluorescence distribution in the cells as DOX–CNGRC. Therefore, we favor the explanation that the uptake of DOX–CNGRC as well as DOX–CARAC is at least partly directed by their physicochemical properties, which determine their passive membrane penetration. The selectivity of the *in vivo* CD13 recognition and targeting [9] may be unrelated to the process of membrane passage of this type of conjugate *in vitro*. Since it is the accessibility and possibly also activation state of the CD13 receptor in the vasculature, which is important for the targeted delivery shown by Arap *et al.* [15], aselectivity at the level of cellular plasma membrane passage may be less important *in vivo* and does not have to be disadvantageous for selectivity of antitumor effect. Also, we cannot yet exclude that for instance a complex involving an integrin or another membrane aminopeptidase (cystinyl aminopeptidase/oxytosinase) would play a role as CNGRC acceptor, although the expression of the latter in endothelial cells has not been described [36,37]. Of interest, it has been shown recently, that a CNGRC conjugate of TNFα increased the antitumor effect of the latter, which was suggested to involve CD13 on angiogenic vessels in cooperation with as yet unknown co-factors [38].

Since the inhibition of CD13 has been suggested to have cell proliferation inhibitory effects in $CD34^{+}CD13^{+}$ hematopoietic progenitors [39] and leukemic cell lines [40] it should be considered whether the CD13 inhibition by DOX–CNGRC as found by us, may contribute to the growth inhibitory effect in HUVEC and tumor cell lines. Although such an effect cannot be excluded completely, it does not seem likely, since we did see only a small enzyme inhibition at the IC_{50} and we did not see a relationship between DOX–CNGRC cytotoxicity and CD13 expression. Since it was recently shown that high concentrations of CD13 inhibitors can inhibit endothelial sprout formation in Matrigel [14] and angiogenesis in a mouse retinal angiogenic model [9] theoretically also moderate inhibition of CD13 by DOX–CNGRC might lead to inhibition of migration and contribute in that way to anti-angiogenic and antitumor effects. One way to envision a mechanism whereby inhibition of CD13 might have anti-angiogenic and antitumor effect is by affecting the proteolytic breakdown of (an) angiogenic inhibitor(s).

In conclusion, DOX has been conjugated via a hydrolysable spacer to the cyclic pentapeptide CNGRC, that has been shown to have tumor endothelial targeting properties because it recognizes *in vivo* CD13, at least in the context of a phage [9,14]. The present conjugate had sufficient stability in human blood for vascular targeting. The uptake in HUVEC or tumor cells leads to an initially predominant cytoplasmic localization, preceding a nuclear localization of fluorescent drug. The *in vitro* antiproliferative effect on endothelial as well as tumor cells was not dependent on the inhibition of CD13 activity, but is more likely caused by intracellularly released DOX. In an *in vivo* experiment no evidence could be found for anincreased antitumor effect of the conjugate in the mouse. The present results contribute to the understanding of the mechanism by which peptide targeted DOX conjugates may interact with tumor and endothelial cells. Clearly more research is needed to establish the optimal chemical requirements of drug–peptide conjugates with regard to stability, recognition by their receptors and mechanism of cytotoxic action.

Acknowledgments

We thank W.J.F. van der Vijgh of our department and R.H. Meloen (Institute for Animal Science and Health, Lelystad) and their teams for help with anthracycline analysis and H. Dekker and C.A.M. Erkelens for excellent technical assistance. This study was supported by the Spinoza-award to H.M.P.

References

[1] Gianni L., Anthracycline resistance: the problem and its definition. Sem. Oncol 1997;24:S10-11–7.

[2] Weiss RB. The anthracyclines: will we ever find a better doxorubicin? Sem Oncol 1992;19:670–86.

[3] Jain RK. Understanding the barriers to drug delivery: high resolution *in vivo* imaging is key. Clin Cancer Res 1999;5:1605–6.

[4] Lankelma J, Dekker H, Fernández Luque R et al. Doxorubicin gradients in human breast cancer. Clin Cancer Res 1999;5:1703–7.

[5] Heijn M, Roberge S, Jain RK. Cellular membrane permeability of anthracyclines does not correlate with their delivery in a tissue isolated tumor. Cancer Res 1999;59:4458–63.

[6] Massing U, Fuxius S. Liposomal formulations of anticancer agents: selectivity and effectiveness. Drug Resistance Updates 2000;3:171–7.

[7] Houba PHJ, Boven E, van der Meulen-Muileman IH, Leenders RGG, Scheeren JW, Pinedo HM, Haisma HJ. Distribution and pharmacokinetics of the prodrug daunorubicin-GA3 in nude mice bearing human ovarian cancer xenografts. Biochem Pharmacol 1999;57:673–80.

[8] Keshet E, Ben-Sasson SA. Anticancer drug targets: approaching angiogenesis. J Clin Invest 1999;104:1497–501.

[9] Pasqualini R, Koivunen E, Kain R et al. Aminopeptidase N is a receptor for tumor-homing peptides and a target for inhibiting angiogenesis. Cancer Res 2000;60:722–7.

[10] Look AT, Ashmun RA, Shapiro LH, Peiper SC. Human myeloid plasma membrane glycoprotein CD13 (gp150) is identical to aminopeptidase N. J Clin Invest 1989;83:1299–307.

[11] Olsen J, Kokholm K, Noren O, Sjostrom H. Structure and expression of aminopeptidase N. Adv Exp Med Biol 1997;421:47–57.

[12] Dixon J, Kaklamanis L, Turley H, Hickson ID, Leek RD, Harris AH, Gatter KC. Expression of aminopeptidase-N (CD13) in normal tissues and malignant neoplasms of epithelial and lymphoid origin. J Clin Pathol 1994;47:43–7.

[13] Kunz J, Krause D, Kremer M, Dermietzel R. The 140-kDa protein of blood-brain barrier-associated pericytes is identical to aminopeptidase N. J Neurochem 1994;62:2375–86.

[14] Bhagwat SV, Lahdenranta J, Giordano R, Arap W, Pasqualini R, Shapiro LH. CD13/APN is activated by angiogenic signals and is essential for capillary tube formation. Blood 2001;97:652–9.

[15] Arap W, Pasqualini R, Ruoslahti E. Cancer treatment by targeted drug delivery to tumor vasculature in a mouse model. Science 1998;279:377–80.

[16] Ellerby HM, Arap W, Ellerby LM, Kain R, Andrusiak R, Del Rio G, Krajewski S, Lombardo CR, Rao R, Ruoslahti E, Bredesen DE, Pasqualini R. Anti-cancer activity of targeted pro-apoptotic peptides. Nature Med 1999;5:1032–8.

[17] Browder T, Butterfield CE, Kräling BM, Shi B, Marshall B, O'Reilly M, Folkman J. Antiangiogenic scheduling of chemotherapy improves efficacy against experimental drug-resistant cancer. Cancer Res 2000;60:1878–86.

[18] Klement G, Baruchel S, Rak J, Man S, Clark K, Hicklin DJ, Bohlen P, Kerbel RS. Continuous low-dose therapy with vinblastine and VEGF receptor-2 antibody induces sustained tumor regression without overt toxicity. J Clin Invest 2000;105:R15–24.

[19] Mross K. Anti-angiogenesis therapy: concepts and importance of dosing schedules in clinical trials. Drug Resistance Updates 2000;3:223–35.

[20] van Hinsbergh VWM, Draijer R. Culture and characterization of human endothelial cells. In: Shaw AJ, editor. Cell culture models of epithelial tissues: a practical approach. Oxford: Oxford University Press, 1996. p. 87–110.

[21] Nagy A, Schally AV, Armatis P, Szepeshazi K, Halmos G, Kovacs M, Zarandi M, Groot K, Miyazaki M, Jungwirth A, Horvath J. Cytotoxic analogs of luteinizing hormone-releasing hormone containing doxorubicin or 2-pyrrolinodoxorubicin, a derivative 500–1000 times more potent. Proc Natl Acad Sci USA 1996;93:7269–73.

[22] Maessen P, Pinedo HM, Mross K, van der Vijgh WJF. New method for the determination of doxorubicin, 4′-epidoxorubicin and all known metabolites in cardiac tissue. J Chromatogr 1988;424:103–10.

[23] De Jong J, Guerand WS, Schoofs WPR, Bast A, van der Vijgh WJF. Simple and sensitive quantification of anthracyclines in mouse atrial tissue using high-performance liquid chromatography and fluorescence detection. J Chromatogr 1991;570:209–16.

[24] Broxterman HJ, Schuurhuis GJ, Lankelma J, Oberink JW, Eekman CA, Claessen AME, Hoekman K, Poot M, Pinedo HM. Highly sensitive and specific detection of P-glycoprotein function for haematological and solid tumour cells using a novel nucleic acid stain. Br J Cancer 1997;76:1029–34.

[25] Favaloro EJ. CD-13 (gp150, aminopeptidase N): co-expression on endothelial and hematopoietic cells with conservation of functional activity. Immunol Cell Biol 1991;69:253–60.

[26] Houba PHJ, Boven E, van der Meulen-Muileman IH, Leenders RGG, Pinedo HM, Haisma HJ. A novel doxorubicin-glucuronide prodrug DOX-GA3 for tumour-selective chemotherapy: distribution and efficacy in experimental human ovarian cancer. Br J Cancer 2001;84:550–7.

[27] Boven E, Schlüper HM, Erkelens CA, Pinedo HM. Doxorubicin compared with related compounds in a nude mouse model for human ovarian cancer. Eur J Cancer 1990;26:983–6.

[28] Leenen PJ, Melis M, Kraal G, Hoogeveen AT, Van Ewijk W. The monoclonal antibody ER-BMDM1 recognizes a macrophage and dendritic cell differentiation antigen with aminopeptidase activity. Eur J Immunol 1992;22:1567–72.

[29] Mechtersheimer G, Moller P. Expression of aminopeptidase N (CD13) in mesenchymal tumors. Am J Pathol 1990;137:1215–22.

[30] Barinaga M. Peptide-guided cancer drugs show promise in mice. Science 1998;279:323–4.

[31] Broxterman HJ, Hoekman K. Direct activation of caspases by RGD-peptides may increase drug sensitivity of tumour cells. Drug Resistance Updates 1999;2:139–41.

[32] De Groot FMH, de Bart ACW, Verheijen JH, Scheeren HW. Synthesis and biological evaluation of novel prodrugs of anthracyclines for selective activation by the tumor-associated protease plasmin. J Med Chem 1999;42:5277–83.

[33] De Groot FMH, van Berkom LWA, Scheeren HW. Synthesis and biological evaluation of 2′-carbamate-linked and 2′-carbonate-linked prodrugs of paclitaxel: selective activation by the tumor-associated protease plasmin. J Med Chem 2000;43:3093–102.

[34] Verheul HMW, Hoekman K, Lupu F, Broxterman HJ, van der Valk P, Kakkar AK, Pinedo HM. Platelet and coagulation activation with vascular endothelial growth factor generation in soft tissue sarcomas. Clin Cancer Res 2000;6:166–71.

[35] Thorén PEG, Persson D, Karlsson M, Nordén B. The antennapodia peptide penetratin translocates a crosslipid bilayers—the first direct observation. FEBS Lett 2000;482:265–8.

[36] Rasmussen TE, Pedraza-Diaz S, Hardre R, Laustsen PG, Carrion AG, Kristensen T. Structure of the human oxytosinase/insulin-regulated aminopeptidase gene and localization to chromosome 5q21. Eur J Biochem 2000;267:2297–306.

[37] Scornik OA, Botbol V. Bestatin as an experimental tool in mammals. Curr Drug Metab 2001;2:67–85.

[38] Curnis F, Sacchi A, Borgna L, Magni F, Gasparri A, Corti A. Enhancement of tumor necrosis factor α antitumor immunotherapeutic properties by targeted delivery to aminopeptidase N (CD13). Nature Biotechnol 2000;18:1185–90.

[39] Rozenzwajg M, Tailleux L, Gluckman JC. CD13/N-aminopeptidase is involved in the development of dendritic cells and macrophages from cord blood $CD34^+$ cells. Blood 2000;95:453–60.

[40] Sekine K, Fujii H, Abe F. Induction of apoptosis by bestatin (ubenimex) in human leukemic cell lines. Leukemia 1999;13:729–34.